

# Density-wave-like gap evolution in $\text{La}_3\text{Ni}_2\text{O}_7$ under high pressure revealed by ultrafast optical spectroscopy

Yanghao Meng,<sup>1,2,\*</sup> Yi Yang,<sup>1,3,\*</sup> Hualei Sun,<sup>4,\*</sup> Sasa Zhang,<sup>3,5</sup> Jianlin Luo,<sup>1</sup>  
Meng Wang,<sup>4,†</sup> Fang Hong,<sup>1,2,6,‡</sup> Xinbo Wang,<sup>1,§</sup> and Xiaohui Yu<sup>1,2,6,¶</sup>

<sup>1</sup>*Beijing National Laboratory for Condensed Matter Physics,*

*Institute of Physics, Chinese Academy of Sciences, Beijing 100190, China*

<sup>2</sup>*School of Physical Sciences, University of Chinese Academy of Sciences, Beijing 100190, China*

<sup>3</sup>*Key Laboratory of Education Ministry for Laser and Infrared System*

*Integration Technology, Shandong University, Qingdao 266237, China*

<sup>4</sup>*Center for Neutron Science and Technology, Guangdong Provincial Key Laboratory of Magnetoelectric Physics and Devices, School of Physics, Sun Yat-Sen University, Guangzhou, China.*

<sup>5</sup>*School of Information Science and Engineering, Shandong University, Qingdao 266237, China*

<sup>6</sup>*Songshan Lake Materials Laboratory, Dongguan, Guangdong 523808, China*

(Dated: May 1, 2024)

We explore the quasiparticle dynamics in bilayer nickelate  $\text{La}_3\text{Ni}_2\text{O}_7$  crystal using ultrafast optical pump-probe spectroscopy at high pressure up to 34.2 GPa. At ambient pressure, the temperature dependence of relaxation indicates appearance of phonon bottleneck effect due to the opening of density-wave-like gap at 151 K. By analyzing the data with RT model, we identified the energy scale of the gap to be 70 meV at ambient pressure. The relaxation bottleneck effect is suppressed gradually by the pressure and disappears around 26 GPa. At high pressure above 29.4 GPa, we discover a new density-wave like order with transition temperature of  $\sim 130$  K. Our results not only provide the first experimental evidence of the density-wave like gap evolution under high pressure, but also offering insight into the underline interplay between the density wave order and superconductivity in pressured  $\text{La}_3\text{Ni}_2\text{O}_7$ .

## I. INTRODUCTION

Nickel-based superconductors have attracted significant interest in physical communities, since first member  $\text{Nd}_{0.8}\text{Sr}_{0.2}\text{NiO}_2$  was discovered[1–4]. Recently,  $\text{La}_3\text{Ni}_2\text{O}_7$  single crystal was found to show a superconducting transition temperature of  $T_c \approx 80$  K at pressures above 14 GPa[5–9].  $\text{La}_3\text{Ni}_2\text{O}_7$  has two layers of nickel oxide ( $\text{NiO}_2$ ) planes in an unit cell, which makes it so special since it can possess a strong interlayer antiferromagnetic coupling between the  $\text{NiO}_2$  planes. This interlayer coupling is believed to be the key to the high-temperature superconductivity, spin density wave (SDW), and antiferromagnetic (AFM) ground state in  $\text{La}_3\text{Ni}_2\text{O}_7$  [10–19].

At ambient pressure.  $\text{La}_3\text{Ni}_2\text{O}_7$  is reported to show metallic behavior. As the temperature is lowered, two density wave (DW) like transitions occur [8, 20–28]. Nuclear magnetic resonance (NMR) [21, 24–26], neutron scattering [29], resonant inelastic X-ray scattering (RIXS)[26] and  $\mu$ -SR experiments [20, 27] showed possible SDW transition around 150 K, accompanied with a striped AFM ground state. Another charge density wave transition was also observed insignificantly through resistance measurements, with  $T_c$  varying from 110 K [5, 23] to 130 K [10, 25] as indicated by a very small

hump in resistance and heat capacity. These transitions were believed to be the result of the competition between  $3d_{x^2-y^2}$  mediated intralayer ferromagnetic coupling and the  $3d_{z^2}$  mediated interlayer antiferromagnetic coupling [11–13]. Upon compression, the so-called charge density wave was reported to vanish quickly upon compression around 3 GPa [9, 10, 25, 27]. However, the spin density wave was confirmed by  $\mu$ -SR below 2.2 GPa [27], after which there is no report about it.

In this work, we report the evolution of DW in  $\text{La}_3\text{Ni}_2\text{O}_7$  under high pressure using ultrafast optical spectroscopy. At ambient pressure, the temperature dependence of relaxation indicates appearance of phonon bottleneck effect due to the opening of density-wave-like gap at 151 K. By analyzing the data with RT model, we identified the energy scale of the gap to be 70 meV, consistent with previous report. The relaxation bottleneck effect is suppressed gradually by the pressure and disappears around 26 GPa. At high pressure above 29.4 GPa, we discover a new density-wave like order with transition temperature of  $\sim 130$  K. Our results not only provide the first experimental evidence of the density-wave like gap evolution under high pressure, but also offering insight into the underline interplay between the density wave order and superconductivity in pressured  $\text{La}_3\text{Ni}_2\text{O}_7$ .

## II. EXPERIMENT

Single-crystalline  $\text{La}_3\text{Ni}_2\text{O}_7$  samples were grown using optical-image floating zone method[5]. The pump-probe setup was described in Ref. [30], where 400 nm pump and

\* These authors contributed equally to this work.

† wangmeng5@mail.sysu.edu.cn

‡ hongfang@iphy.ac.cn

§ xinbowang@iphy.ac.cn

¶ yuxh@iphy.ac.cn

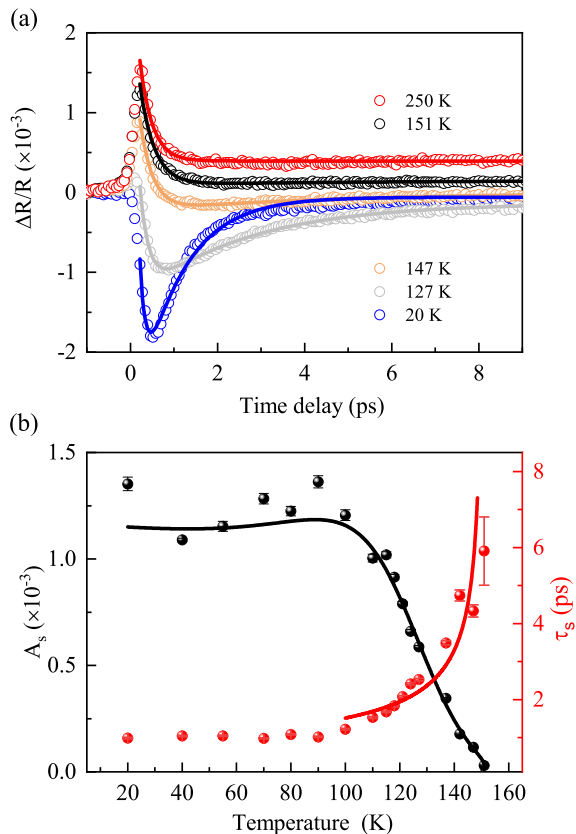


FIG. 1. (a)  $\Delta R / R$  signals at several selected temperatures and ambient pressure. The solid lines are the fitting curves. (b) Temperature dependent amplitude  $A_s$  and relaxation time  $\tau_s$ . The solid lines are fitting results according to RT model.

800 nm probe pulses with 60 fs pulse width and 50 kHz repetition rate were used. High pressure was generated by screw-pressure-type diamond anvil cell (DAC) with a 500- $\mu\text{m}$  culet. The sample chamber with a diameter of 300  $\mu\text{m}$  was made in a Rhenium gasket. A small piece of  $\text{La}_3\text{Ni}_2\text{O}_7$  crystal was loaded in the center of the chamber and a ruby ball was placed aside the sample. Fine KBr powders were employed as the pressure transmitting medium which could provide a quasi-hydrostatic environment up to 31 GPa in DAC[30]. The DAC was loaded in a cryostat with an optical window for the temperature dependent measurements. An additional thermal sensor was mounted on the force plate of the DAC for more precise measurement of sample temperature. Pressure was calibrated using the ruby fluorescence shift at low temperature for all experiments. Both beams were focused onto sample surface using a 5x objective lens, giving pump and probe fluences of 45  $\mu\text{J}/\text{cm}^{-2}$  and 9  $\mu\text{J}/\text{cm}^{-2}$ , respectively.

### III. RESULTS AND DISCUSSION

Figure 1(a) shows the time-resolved reflectivity change  $\Delta R/R$  in  $\text{La}_3\text{Ni}_2\text{O}_7$  at several selected temperatures and near ambient pressure. At high temperatures, photoexcitation leads to a quick rise in the reflectivity, followed by a fast decay into a constant offset with a relaxation time change slightly as temperature is increased to 250 K. Below  $T_{DW} \sim 151$  K, an additional long-lived component with negative amplitude appears, which relaxes faster with increases in amplitude with further decreasing temperature resulting in the initial positive change of  $\Delta R/R$  turns to negative. Therefore, we ascribe the fast-decay signal to the electron-phonon thermalization and the slow-decay component to the recombination across the density-wave-like gap. Accordingly, we fit the data using a single-component exponential function,  $\Delta R/R = A_f e^{-t/\tau_f} + C$  above  $T_{DW}$ , and two-component decay function,  $\Delta R/R = A_f e^{-t/\tau_f} - A_s e^{-t/\tau_s} + C$  at low temperature, where  $A$  and  $\tau$  represent the relaxation amplitude and decay time, respectively. The subscripts ( $f$  and  $s$ ) denote the fast and slow relaxation processes and  $C$  is a constant offset. The experimental data can be fitted quite well as shown in Fig. 1(a). The extracted  $A_s$  and  $\tau_s$  as function of temperature are plotted in Fig. 1(b). We see that below  $T_{DW}$ ,  $A_s$  increases sharply from zero, while  $\tau_s$  shows a continuous divergence. The anomalous behavior can be explained by a relaxation bottleneck associated with the opening of a density-wave like gap, as will be discussed in detail later.

Here, we employ the Rothwarf-Taylor (RT) model to explain the slow relaxation process in  $\text{La}_3\text{Ni}_2\text{O}_7$  [31]. It is a phenomenological model was initially proposed to describe the relaxation of photoexcited superconductors, where the formation of a gap in the electronic density of states creates a relaxation bottleneck of the photoexcited quasiparticles. The recombination is dominated by the emission and reabsorption of the high frequency phonons whose decay determines the recovery of photoexcited quasiparticles back to the equilibrium states. The RT model has also been demonstrated to be applicable for other systems with gap opening in the density of states, such as charge/spin density wave, and heavy fermion[32–34]. Based on this model, the thermally quasiparticle density  $n_T$  is related to the transient reflectivity amplitude  $A$  via  $n_T \propto [A(T)/A(T \rightarrow 0)]^{-1} - 1$ . Combining the relationship of  $n_T \propto \sqrt{\Delta(T)T} \exp[-\Delta(T)/T]$ , we obtain [35]:

$$A(T) \propto \frac{\Phi / (\Delta(T) + k_B T / 2)}{1 + \gamma \sqrt{2k_B T / \Delta(T)} \exp[-\Delta(T)/k_B T]} \quad (1)$$

where the  $\Phi$  is the pump fluence,  $\Delta(T)$  is the temperature dependence of gap energy,  $k_B$  is the Boltzmann constant, and  $\gamma$  is a fitting parameter. In the RT model, the relaxation time near transition temperature is dominated by phonons with frequency  $\omega > 2\Delta$  transferring their en-

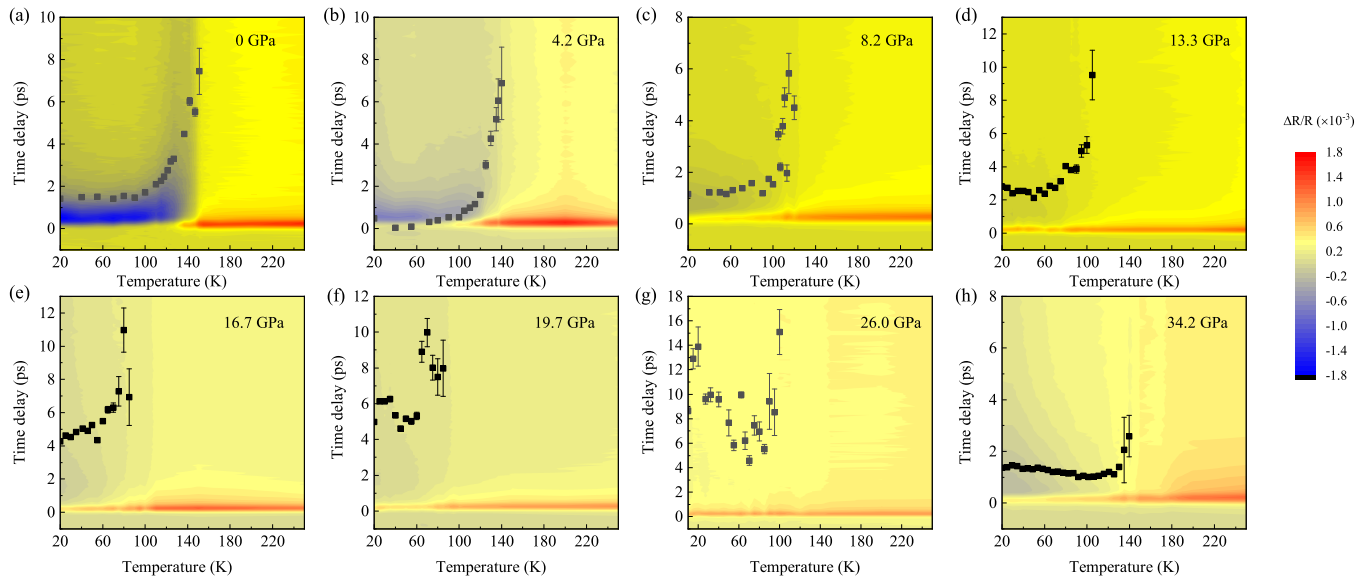


FIG. 2. Temperature dependent pump probe spectra taken at (a) 0 GPa, (b) 4.2 GPa, (c) 8.2 GPa, (d) 13.3 GPa, (e) 16.7 GPa, (f) 19.7 GPa, (g) 26 GPa and (h) 34.2 GPa. The scatters in each panel are the extracted  $\tau_s$ .

ergy to lower frequency phonons with  $\omega < 2\Delta$ , so the excitation of the condensed quasiparticles would stop. The relaxation time  $\tau$  is associated with  $n_T$  as well and is given by [35]:

$$\tau^{-1}(T) = \Gamma[\delta + 2n_T][\Delta(T) + \alpha T\Delta(T)^4], \quad (2)$$

where  $\Gamma$ ,  $\delta$  and  $\alpha$  are temperature independent fitting parameters, with  $\alpha$  having an upper limit of  $52/(\theta_D^3 T_{min})$ ,  $\theta_D$  is the Debye temperature, and  $T_{min}=20$  K is the minimum temperature of the experiment. Assuming that  $\Delta(T)$  obeys BCS temperature dependence, we fit the  $A_s$  and  $\tau_s$  using Eq.(1) and (2). The results are shown as the solid lines in Fig.1(b). From the fit we obtain the transition temperature  $T_{DW} \sim 151$  K and the gap energy  $\Delta(0) \sim 70$  meV, corresponding to  $\Delta(0) = 5.4k_B T_{DW}$ , which is in good agreement with the values previously reported by optical conductivity, ARPES and NMR spectroscopy [21, 24–26]. The excellent fits strongly support our assumption of the formation of a gap in the electric density of states due to the development of density-wave-like long range order below  $T_{DW}$ .

To further track the evolution of gap amplitude in  $\text{La}_3\text{Ni}_2\text{O}_7$  as a function of pressure, we perform ultra-fast pump-probe measurements under high pressure up to 34.2 GPa in DAC. Fig. 2 displays the temperature dependent transient reflectivity data at several selected pressures. We immediately notice that the slow relaxation component with negative amplitude survives only at temperature below  $T_{DW}$ . We employ similar fitting procedures described above to the experimental data under various pressures and plot the fitting parameter  $\tau_s$

as scatters in Fig. 2. Interestingly, the feature of gap opening, that is the divergence of  $\tau_s$  progressively degenerates and weakens before disappears completely around 26 GPa. It is worth nothing that although the phonon bottleneck effect is absent at 26 GPa, the slow relaxation component with negative amplitude survives up to 95 K. Above 29.4 GPa, the relaxation time  $\tau_s$  decreases slightly with increasing temperature and then exhibits a divergence behavior at  $T_{DW}$ . Such a temperature dependence of  $\tau_s$  is similar to that at near ambient pressure strongly suggesting the re-opening of energy gap in the density of states under pressure above 29.4 GPa.

In order to obtain detailed information of the gap evolution, the  $\Delta R/R$  signals as a function of pressure at 20 K are plotted in Fig.3(a). The negative amplitude monotonically reduces with increasing pressure and becomes indistinguishable at 26 GPa above which the negative signal appears again. Fig. 3(b) displays the fitting parameters  $A_s$  and  $\tau_s$  as a function of pressure at 20 K. As the pressure increases up to 2.2 GPa,  $A_s$  drops dramatically, accompanied by a slight decrease of  $\tau_s$ . Upon further compression,  $A_s$  decreases gradually towards zero while  $\tau_s$  exhibits a quasi-divergence around 26 GPa. According to Eq.(2), the relaxation time increases with the decrease of  $\Delta$  at fixed temperature and vice versa. Therefore, we can infer that the increase of  $\tau_s$  with increasing pressure is due to the progressive suppression of density wave gap in this pressure range. Above 29.4 GPa, the increase of  $A_s$  and decrease of  $\tau_s$  are in line with the RT model where the presence of energy gap leads to a relaxation bottleneck.

The identical RT analysis was applied to the temperature dependence of the slow relaxation  $\tau_s$  and  $A_s$ [36]

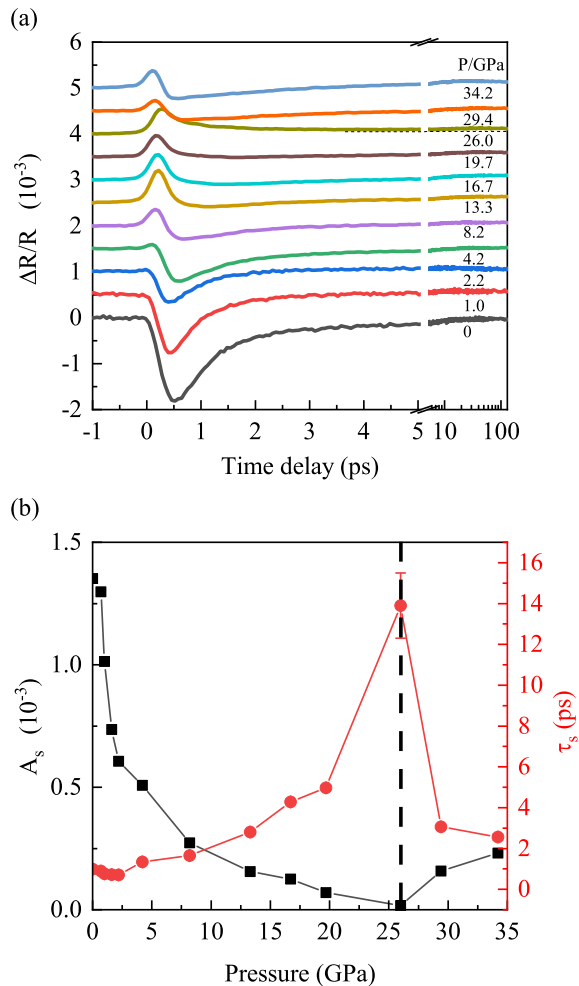


FIG. 3. (a) Pump-probe spectra at various pressures at 20 K. (b) The extracted amplitude  $A_s$  and decay time  $\tau_s$ .

under various pressures except that at 26 GPa. The extracted  $T_{DW}$  values are summarized in the temperature-pressure phase diagram in Fig. 4. Based on the above high pressure results, the diagram can be divided into two major regions with a critical pressure of 26 GPa, which are labeled as the density wave like order I and II (labeled as DW I and DW II). In the low pressure region, the density wave transition is gradually suppressed from  $T_{DW} \approx 151$  K near AP to  $T_{DW} \approx 110$  K at 13.3 GPa. The value of  $T_{DW}$  rapidly decreases to around 95 K at 16.7 GPa and then remains almost constant with pressure up to 19.7 GPa. Since no phonon bottleneck effect is observed at 26 GPa, a value of 95 K, at which the negative decay component disappears, is added into Fig. 4 as a hollow circle. Upon further increasing pressure, typical divergent behavior of  $\tau_s$  appears again near 135 K, suggesting the presence of another energy gap in the density of states. The transition temperature increases slightly with further increasing pressure.

The present work gives an unambiguous fact that there is a gap opening in the density of states in  $\text{La}_3\text{Ni}_2\text{O}_7$  un-

der pressure indicating that the pump-probe technique is sensitive to the presence of density wave like order. However, we can not distinguish whether it is a spin or charge density wave which is still under debate and needs further investigation. Upon compression, the density wave order is gradually suppressed, leading to the decrease of the gap amplitude from  $\sim 70$  meV at AP to  $\sim 20$  meV at 13.4 GPa above which it remains constant before vanishing at 26 GPa. In this pressure range, short-range density wave order may partially exist and induce small energy gaps at different parts of Fermi surface below  $T_{DW}$ . Additionally, the emergence of a new density-wave like order under pressure beyond 29.4 GPa is probably related to the charge density wave order as proposed by the theoretical results. The energy scale of this gap is about 25 meV which increases slightly with further increase pressure. Although superconductivity with transition temperature of 80 K under pressure above 14 GPa has been reported, we do not observe any signature of superconductivity probably due to the low superconducting volume in this nickelate. Our results reveal that both the density wave like orders coexist with the superconductivity, while it competes with superconductivity in the DW I region which is similar to the cuprates and iron-based superconductors[33, 37].

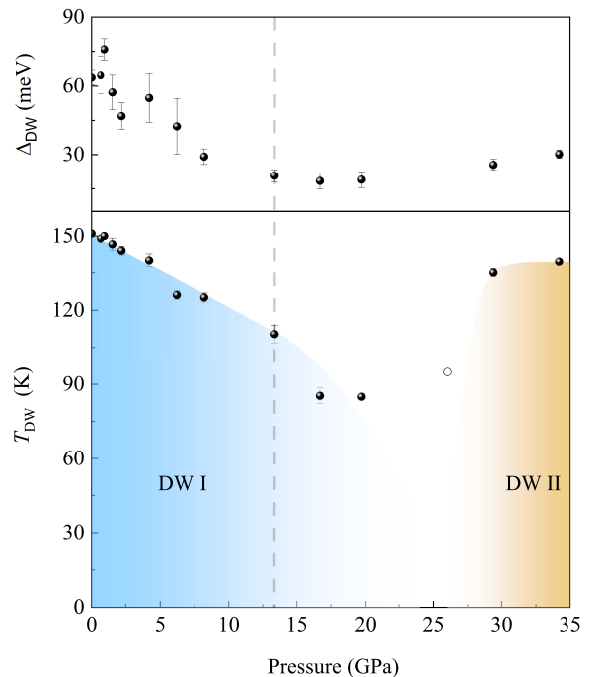


FIG. 4. Temperature-pressure phase diagram of the  $\text{La}_3\text{Ni}_2\text{O}_7$  based on the pump probe spectroscopy measurements. The upper panel shows the evolution of the extracted gap as a function of pressure.

#### IV. CONCLUSION

In summary, we have performed ultrafast pump-probe measurements on single crystalline  $\text{La}_3\text{Ni}_2\text{O}_7$  under pressure up to 34.2 GPa. At ambient pressure, the temperature dependence of relaxation indicates appearance of phonon bottleneck effect due to the opening of density-wave like gap at 151 K. By analyzing the data with RT model, we identified the energy scale of the gap to be 70 meV, consistent with previous report. The relaxation bottleneck effect is suppressed gradually by the pressure and disappears around 26 GPa. At high pressure above 29.4 GPa, we discover a new density-wave like order with

transition temperature of  $\sim 130$  K. Our results not only provide the first experimental evidence of the density-wave like gap evolution under high pressure, but also offering insight into the underline interplay between the density wave order and superconductivity in pressured  $\text{La}_3\text{Ni}_2\text{O}_7$ .

#### ACKNOWLEDGMENTS

This work was supported by the National Natural Science Foundation of China (Grant Nos. 11974414) and the Synergetic Extreme Condition User Facility (SECUF).

- 
- [1] D. Li, K. Lee, B. Y. Wang, M. Osada, S. Crossley, H. R. Lee, Y. Cui, Y. Hikita, and H. Y. Hwang, Superconductivity in an infinite-layer nickelate, *Nature* **572**, 624 (2019).
- [2] S. Zeng, C. Li, L. E. Chow, Y. Cao, Z. Zhang, C. S. Tang, X. Yin, Z. S. Lim, J. Hu, P. Yang, and A. Ariando, Superconductivity in infinite-layer nickelate  $\text{La}_{1-x}\text{Ca}_x\text{NiO}_2$  thin films, *Science Advances* **8**, eabl9927 (2022).
- [3] M. Osada, B. Y. Wang, K. Lee, D. Li, and H. Y. Hwang, Phase diagram of infinite layer praseodymium nickelate  $\text{Pr}_{1-x}\text{Sr}_x\text{NiO}_2$  thin films, *Physical Review Materials* **4**, 121801 (2020).
- [4] M. Osada, B. Y. Wang, B. H. Goodge, S. P. Harvey, K. Lee, D. Li, L. F. Kourkoutis, and H. Y. Hwang, Nickelate superconductivity without rare-earth magnetism:  $(\text{La}, \text{Sr})\text{NiO}_2$ , *Advanced Materials* **33**, 2104083 (2021).
- [5] H. Sun, M. Huo, X. Hu, J. Li, Z. Liu, Y. Han, L. Tang, Z. Mao, P. Yang, B. Wang, *et al.*, Signatures of superconductivity near 80 k in a nickelate under high pressure, *Nature* **621**, 493 (2023).
- [6] K. Jiang, Z. Wang, and F.-C. Zhang, High temperature superconductivity in  $\text{La}_3\text{Ni}_2\text{O}_7$ , arXiv preprint arXiv:2308.06771 (2023).
- [7] Y. Zhou, J. Guo, S. Cai, H. Sun, P. Wang, J. Zhao, J. Han, X. Chen, Q. Wu, Y. Ding, *et al.*, Evidence of filamentary superconductivity in pressurized  $\text{La}_3\text{Ni}_2\text{O}_7$  single crystals, arXiv preprint arXiv:2311.12361 (2023).
- [8] P. Puphal, P. Reiss, N. Enderlein, Y.-M. Wu, G. Khalullin, V. Sundaramurthy, T. Priessnitz, M. Knauft, L. Richter, M. Isobe, *et al.*, Unconventional crystal structure of the high-pressure superconductor  $\text{La}_3\text{Ni}_2\text{O}_7$ , arXiv preprint arXiv:2312.07341 (2023).
- [9] G. Wang, N. N. Wang, X. L. Shen, J. Hou, L. Ma, L. F. Shi, Z. A. Ren, Y. D. Gu, H. M. Ma, P. T. Yang, Z. Y. Liu, H. Z. Guo, J. P. Sun, G. M. Zhang, S. Calder, J.-Q. Yan, B. S. Wang, Y. Uwatoko, and J.-G. Cheng, Pressure-induced superconductivity in polycrystalline  $\text{La}_3\text{Ni}_2\text{O}_{7-\delta}$ , *Phys. Rev. X* **14**, 011040 (2024).
- [10] G. Wang, N. Wang, J. Hou, L. Ma, L. Shi, Z. Ren, Y. Gu, X. Shen, H. Ma, P. Yang, *et al.*, Pressure-induced superconductivity in polycrystalline  $\text{La}_3\text{Ni}_2\text{O}_7$ , arXiv preprint arXiv:2309.17378 (2023).
- [11] Z. Luo, X. Hu, M. Wang, W. Wú, and D.-X. Yao, Bilayer two-orbital model of  $\text{La}_3\text{Ni}_2\text{O}_7$  under pressure, *Phys. Rev. Lett.* **131**, 126001 (2023).
- [12] V. Christiansson, F. Petocchi, and P. Werner, Correlated electronic structure of  $\text{La}_3\text{Ni}_2\text{O}_7$  under pressure, *Phys. Rev. Lett.* **131**, 206501 (2023).
- [13] F. Lechermann, J. Gondolf, S. Bötzel, and I. M. Eremin, Electronic correlations and superconducting instability in  $\text{La}_3\text{Ni}_2\text{O}_7$  under high pressure, *Phys. Rev. B* **108**, L201121 (2023).
- [14] Y. Gu, C. Le, Z. Yang, X. Wu, and J. Hu, Effective model and pairing tendency in bilayer ni-based superconductor  $\text{La}_3\text{Ni}_2\text{O}_7$ , arXiv preprint arXiv:2306.07275 (2023).
- [15] X. Chen, P. Jiang, J. Li, Z. Zhong, and Y. Lu, Critical charge and spin instabilities in superconducting  $\text{La}_3\text{Ni}_2\text{O}_7$ , arXiv preprint arXiv:2307.07154 (2023).
- [16] D. Shilenko and I. Leonov, Correlated electronic structure, orbital-selective behavior, and magnetic correlations in double-layer  $\text{La}_3\text{Ni}_2\text{O}_7$  under pressure, arXiv preprint arXiv:2306.14841 (2023).
- [17] C. Lu, Z. Pan, F. Yang, and C. Wu, Interplay of two  $e_g$  orbitals in superconducting  $\text{La}_3\text{Ni}_2\text{O}_7$  under pressure, arXiv preprint arXiv:2310.02915 (2023).
- [18] H. Lange, L. Homeier, E. Demler, U. Schollwöck, F. Grusdt, and A. Bohrdt, Feshbach resonance in a strongly repulsive bilayer model: a possible scenario for bilayer nickelate superconductors, arXiv preprint arXiv:2309.15843 (2023).
- [19] Y. Zhang, L.-F. Lin, A. Moreo, and E. Dagotto, Electronic structure, dimer physics, orbital-selective behavior, and magnetic tendencies in the bilayer nickelate superconductor  $\text{La}_3\text{Ni}_2\text{O}_7$  under pressure, *Phys. Rev. B* **108**, L180510 (2023).
- [20] K. Chen, X. Liu, J. Jiao, M. Zou, Y. Luo, Q. Wu, N. Zhang, Y. Guo, and L. Shu, Evidence of spin density waves in  $\text{La}_3\text{Ni}_2\text{O}_{7-\delta}$ , arXiv preprint arXiv:2311.15717 (2023).
- [21] Z. Dan, Y. Zhou, M. Huo, Y. Wang, L. Nie, M. Wang, T. Wu, and X. Chen, Spin-density-wave transition in double-layer nickelate  $\text{La}_3\text{Ni}_2\text{O}_7$ , arXiv preprint arXiv:2402.03952 (2024).
- [22] G. Wu, J. Neumeier, and M. Hundley, Magnetic susceptibility, heat capacity, and pressure dependence of the electrical resistivity of  $\text{La}_3\text{Ni}_2\text{O}_7$  and  $\text{La}_4\text{Ni}_3\text{O}_{10}$ , *Physical Review B* **63**, 245120 (2001).
- [23] Z. Liu, H. Sun, M. Huo, X. Ma, Y. Ji, E. Yi, L. Li, H. Liu, J. Yu, Z. Zhang, *et al.*, Evidence for charge and spin order

- in single crystals of  $la_3ni_2o_7$  and  $la_3ni_2o_6$ , arXiv preprint arXiv:2205.00950 (2022).
- [24] T. Fukamachi, Y. Kobayashi, T. Miyashita, and M. Sato,  $^{139}La$  nmr studies of layered perovskite systems  $la_3ni_2o_{7-\delta}$  and  $la_4ni_3o_{10}$ , *Journal of Physics and Chemistry of Solids* **62**, 195 (2001).
- [25] M. Kakoi, T. Oi, Y. Ohshita, M. Yashima, K. Kuroki, Y. Adachi, N. Hatada, T. Uda, and H. Mukuda, Multi-band metallic ground state in multilayered nickelates  $la_3ni_2o_{7-\delta}$  and  $la_4ni_3o_{10}$  revealed by  $^{139}La$  - nmr at ambient pressure, arXiv preprint arXiv:2312.11844 (2023).
- [26] K.-J. Zhou, X. Chen, J. Choi, Z. Jiang, J. Mei, K. Jiang, J. Li, S. Agrestini, M. Garcia-Fernandez, H. Sun, *et al.*, Electronic and magnetic excitations in  $la_3ni_2o_7$ , DOI: <https://doi.org/10.21203/rs.3.rs-3901266/v1> (2024).
- [27] R. Khasanov, T. J. Hicken, D. J. Gawryluk, L. P. Sorel, S. Bötzel, F. Lechermann, I. M. Eremin, H. Luetkens, and Z. Guguchia, Pressure-induced split of the density wave transitions in  $la_3ni_2o_{7-\delta}$ , arXiv preprint arXiv:2402.10485 (2024).
- [28] T. Cui, S. Choi, T. Lin, C. Liu, G. Wang, N. Wang, S. Chen, H. Hong, D. Rong, Q. Wang, *et al.*, Strain-mediated phase crossover in ruddlesden–popper nickelates, *Communications Materials* **5**, 32 (2024).
- [29] C. D. Ling, D. N. Argyriou, G. Wu, and J. Neumeier, Neutron diffraction study of  $La_3Ni_2O_7$ : Structural relationships among  $n=1, 2$ , and  $3$  phases  $La_{n+1}Ni_nO_{3n+1}$ , *Journal of Solid State Chemistry* **152**, 517 (2000).
- [30] Y. Yang, Y. H. Meng, B. R. Lu, F. Jin, Y. G. Shi, F. Hong, S. S. Zhang, X. H. Yu, X. B. Wang, and J. L. Luo, Ultrafast carrier and phonon dynamics in  $bi_2se_3$  under high pressure, *Phys. Rev. B* **109**, 064307 (2024).
- [31] A. Rothwarf and B. N. Taylor, Measurement of recombination lifetimes in superconductors, *Phys. Rev. Lett.* **19**, 27 (1967).
- [32] J. Demsar, B. Podobnik, V. V. Kabanov, T. Wolf, and D. Mihailovic, Superconducting gap  $\Delta_c$ , the pseudogap  $\Delta_p$ , and pair fluctuations above  $T_c$  in overdoped  $y_{1-x}Ca_xba_2cu_3o_7 - \delta$  from femtosecond time-domain spectroscopy, *Phys. Rev. Lett.* **82**, 4918 (1999).
- [33] E. E. M. Chia, D. Talbayev, J.-X. Zhu, H. Q. Yuan, T. Park, J. D. Thompson, C. Panagopoulos, G. F. Chen, J. L. Luo, N. L. Wang, and A. J. Taylor, Ultrafast pump-probe study of phase separation and competing orders in the underdoped  $(Ba, K)fe_2as_2$  superconductor, *Phys. Rev. Lett.* **104**, 027003 (2010).
- [34] D. F. M. F. P. Claudio Giannetti, Massimo Capone and D. Mihailovic, Ultrafast optical spectroscopy of strongly correlated materials and high-temperature superconductors: a non-equilibrium approach, *Advances in Physics* **65**, 58 (2016).
- [35] V. V. Kabanov, J. Demsar, B. Podobnik, and D. Mihailovic, Quasiparticle relaxation dynamics in superconductors with different gap structures: Theory and experiments on  $YBa_2Cu_4O_{7-\delta}$ , *Phys. Rev. B* **59**, 1497 (1999).
- [36] See Supplemental Material for the pump-probe spectra of all pressures, fitted results, and Raman spectra illustration in inhomogenous oxygen stoichiometry.
- [37] L. Taillefer, Scattering and pairing in cuprate superconductors, *Annual Review of Condensed Matter Physics* **1**, 51 (2010).